Mechanical Systems and Signal Processing (2003) **17**(2), 273–283
doi:10.1006/mssp.2002.1531, available online at http://www.idealibrary.com on IDEAL®

FAULT DETECTION IN GEAR DRIVES WITH NON-STATIONARY ROTATIONAL SPEED — PART II: THE TIME–QUEFRENCY APPROACH

G. Meltzer

Technical Diagnostics, Department of Energy Machines and Machine Laboratory, Faculty of Mechanical Engineering, Dresden University of Technology, D-01062 Dresden, Germany.
E-mail: meltzer@mal.mw.tu-dresden.de

AND

Yu.Ye. Ivanov

ZF Friedrichshafen, Germany

(Received 1 February 1999, accepted in revised form 23 September 2002)

This paper deals with the recognition of faults in toothing during non-stationary start up and run down of gear drives. In the first part, this task was solved by means of the time–frequency analysis. A planetary gear was used as a case study. Part II contains a new approach using the time–quefrency analysis. The same example was successfully subjected in this procedure.

1. INTRODUCTION

The appearance of sidebands in the frequency spectrum of measured structure-borne noise of gear cases is, according to our present knowledge, a sure symptom for faults in toothing. These sidebands are generated by the amplitude modulation or frequency modulation, resp. of the meshing vibrations, as a result of meshing of faulty teeth [1,2]. The sideband analysis was executed by means of the classical Fourier analysis as well as—because of the non-stationarity of rotational speed during measuring—also by means of the time–frequency analysis. Depending on the chosen time and frequency resolutions the contour plots of time–frequency distribution (TFD) shows more wavy lines (representing the instantaneous frequency), dots on straight lines (representing the instantaneous amplitude) or parallel straight frequency lines (representing the meshing frequency and sidebands). The last-mentioned analysis was used in Part I of our paper [3] and tested as an approach for fault diagnostics in gearboxes.

The ordering spectrum as the result of Fourier transformation of the angle-equidistant sampled measured signal shows the order of teeth meshing (this is equal to the number of teeth multiplied with the rotational frequency of the shaft) accompanied by some sidebands around the meshing frequency. In the plot of time-ordering distribution (TOD), these sidebands marked perpendicularly orientated straight lines. The spacing of sidebands to the meshing order is a symptom for the location of the fault. Therefore, these distances had to be determined very carefully. For doing this, we applied the well-known tool of cepstral analysis. A cepstrum is the inverse Fourier-transformed logarithm of the belonging-to spectrum [1, 2]. Periodically located sidebands in the spectrum are

0888–3270/03/ + $30.00/0

characterised by particular peaks in the cepstrum. The simultaneous appearance of two peaks in the cepstrum with quefrencies correlates to the rotational speed of central gear and annulus of second planetary detected toothing faults or damages at the central gear as well as at the annulus [3].

A similar tool for exact recognition and following the precise identification of sideband spacings out from TFD in the case of non-stationary rotational speed was not available until now. But there exists a necessity for this, in order to solve the following problem: How can the existence of gear fault be detected in the case of continuously changing rotational speed? In gear drives, the sideband distance changes with the rotational speed of the damaged wheels [1, 4]. Any unsteady rotational speed consequently generates time-dependent sideband spacings. In this case, the application of the ordinary Fourier cepstrum is not suitable because of the expected 'smearing over' of the cepstral peaks. Therefore, it seems to be unable to identify the toothing faults outgoing from time-equidistant sampled measuring values [3]. On the other side, the TFD has shown these sidebands at the planetary set 2 clearly enough.

To avoid the implementation of a phase angle encoder (please remember: sampling in small angle intervals would be an easy approach for solving our task, but it is connected with more hardware expense), we have to find an until-now-missed method for transformation of the TFD by a 'time quefrency analysis' (TQA) into a time–quefrency distribution (TQD) in order to identify the sideband distances also quantitatively. Our target was now to create and to apply such a new tool on the basis of the time-equidistant sampled measuring data. We have done this successfully—about the result will be reported furthermore.

2. THE METHOD OF TIME–QUEFRENCY ANALYSIS

We are concerned here with quadratic time–frequency distributions $TFD_X(t;\omega)$ of Cohen class which fulfil the condition

$$|X(j\omega)|^2 = \int_{-\infty}^{+\infty} TFD_x(t;\omega)\,\mathrm{d}t \tag{1}$$

with $|X(j\omega)|^2$ as the square of magnitude of the Fourier-transformed signal [5–7].

Equation (1) shows that the Fourier powerspectrum can be reconstructed out of the TFD of the belonging-to signal. By executing the logarithm and subsequently the inverse Fourier transformation of both sides of equation (1) we get

$$C_x(\tau) = \int_{-\infty}^{+\infty} \ln\left[\int_{-\infty}^{+\infty} TFD_x(t;\omega)\,\mathrm{d}t\right] \exp(j\omega\tau)\,\mathrm{d}\omega \tag{2}$$

with $C_X(\tau)$ as the ordinary Fourier power cepstrum of $x(t)$:

$$C_x(\tau) = \int_{-\infty}^{+\infty} \ln|X(j\omega)|^2 \exp(j\omega\tau)\,\mathrm{d}\omega. \tag{3}$$

Equations (2) and (3) show that on the premise of equation (1) also the Fourier cepstrum can be reconstructed from the time–frequency distribution $TFD_X(t;\omega)$.

We want to define a new transformation similar to equation (3), in which the Fourier-power spectrum shall be replaced by the time-dependent power spectrum or the time–frequency distribution $TFD_X(t;\omega)$:

$$CTQD_x(t;\tau) = \int_{-\infty}^{+\infty} \ln[TFD_x(t;\omega)] \exp(\mathrm{j}\omega\tau)\,\mathrm{d}\omega. \tag{4}$$

The left side of equation (4) is the inverse Fourier-transformed of logarithm of the time–frequency distribution $TFD_X(t;\omega)$. It depends on two variables: the time t and the quefrency τ. Therefore, it can be named the TQD.

The inverse Fourier transformation (3) is used for detection of periodic components of the spectrum $|X(j\omega)|^2$ of signal $x(t)$. The inverse Fourier transformation (4) gives the same insight, but additionally it shows these periodicities in the frequency domain $\boldsymbol{\omega}$ as functions of time. Because of it, the new created function $CTQD_X(t;\tau)$ can be coordinated to the class of cepstral functions as a TQD. It shows the momentary cepstrum of $x(t)$, which depends generally on time and which can be favourably used for a quantitative identification of transient periodicities on frequency in the spectrum of $x(t)$. It can be also averaged over the time to the time-averaged cepstrum. The result is

$$G_x(\tau) = \int_{-\infty}^{+\infty} CTQD_x(t;\tau)\,\mathrm{d}t. \tag{5}$$

Equation (5) is similar to equation (2): both are time-independent cepstra. But nevertheless, they are not identical: $C_X(\tau) \neq G_X(\tau)$. This can be proved by substitution of equation (4) into (5) with the result (6) and following comparison with equation (2):

$$G_x(\tau) = \int_{-\infty}^{+\infty} \left[\int_{-\infty}^{+\infty} \ln[TFD_x(t;\omega)] \exp(j\omega\tau)\,\mathrm{d}\omega \right] \mathrm{d}t. \tag{6}$$

We lost the identity by changing the sequence of the operations of logarithm and integration in equations (2) and (6), resp. The conclusion is that the Fourier power cepstrum $C_X(\tau)$ cannot be reconstructed outgoing from the special form of TQD, which is formulated in equation (5) as $CTQD_X(t;\tau)$.

The mutual relations between spectrum, cepstrum, TFD and TQD are shown in Fig. 1.

Now something about the properties of the new created class of TQD.

It is well known that the Fourier power cepstrum $C_X(\tau)$ is a function of quefrency τ with real function quantities only. This is caused by the circumstance that the Fourier spectrum $|X(j\omega)|^2$ is an even function of $\boldsymbol{\omega}$. Also the mostly used representants of Cohen class, the Wigner–Ville distribution (WVD) and the Choi–Williams distribution (CWD) are even functions of ω: $TFD_X(t;\omega) = TFD_X(t;-\omega)$ [6]. But nevertheless, the time–quefrency distribution $CTQD_X(t;\tau)$ is generally a function with complex function quantities. This is caused by the logarithmic operation of the TFD in equation (4), which provides not always positive function quantities. This is marked by the first capital 'C' of the abbreviation CTQD. In the case of only positive function quantities of TFD ($TFD_X(t;\omega) > 0$ for arbitrary t, ω) we get a TQD with only real function quantities.

Only few of TFD of Cohen class possess the so-called 'positivity' [5]. But in the general case, the signal terms of TFD are always positive or zero, and only the interference terms can be also negative [6, 7]. After a radical smoothing of interference terms by means of a

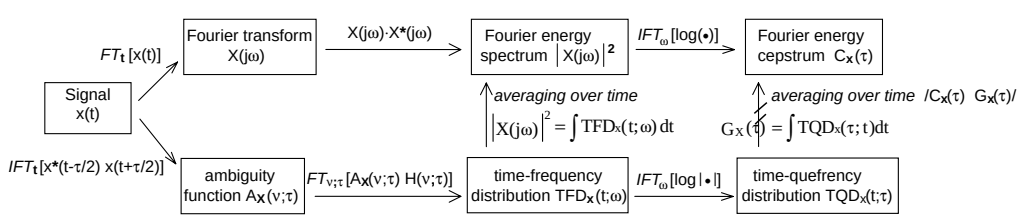

Figure 1. Mutual relations between all transformations of a measured signal and distributions in frequency, quefrency, time–frequency, time–quefrency and ambiguity domain.

well chosen smoothing kernel, the negative terms almost vanish and we can consider the TFD as 'nearly positive'. Therefore, we can replace the $TFD_X(t;\omega)$ in equation (4) by its magnitude:

$$TQD_x(t;\tau) = \int_{-\infty}^{+\infty} \ln|TFD_x(t;\omega)| \exp(j\omega\tau)\,\mathrm{d}\omega. \tag{7}$$

Using equation (7) instead of equation (4) we can economise a lot of calculating time by renunciation of complex algebra. The time averaging of $TQD_X(t;\omega)$ can be done subsequently with formula (5).

According to equations (4) and (7) for every representant of Cohen class TFD we can find an appropriate TQD. All these are members of a new class of distributions in the time–quefrency domain.

In the next section, an application of the described new TQD will be shown. We will detect and identify time-independent (Section 3.1) and time-dependent (Section 3.2) periodicities of sidebands in the measured acceleration of a gearcase of a passenger car [3]. The TQD proves to be a strong tool for the recognition of toothing faults or damages during test runs with fast-changing rotational speed here.

3. APPLICATION OF TQD FOR GEAR DRIVE DIAGNOSTICS

The investigated manual-controlled gearbox of a passenger car as well as the experiments are described in Part I of our paper [3].

3.1. TQA OF ANGLE-EQUIDISTANT SAMPLED MEAUSURED DATAS

The central part of Fig. 2 shows the contour plot of the CWD of the angle-equidistant sampled measured signal of structure-borne noise at the gear housing. You can see the time function in the left part and the ordering spectrum at the bottom of the same figure. Figure 3 shows the time–quefrency distribution $TQD_X(t;\tau)$, which was calculated by the inverse Fourier-transformation of the logarithm of magnitude of CWD according to equation (7). Some vertical straight lines can be recognised. The dominating ones at the 0.327th and the 0.527th-order quefrency belong to the rotational speed of the central gear and annulus of the second planetary set, resp. These cepstral lines characterise corresponding sidebands in the frequency domain and modulations in the time domain. All these properties are symptoms for existing faults or damages in these gear wheels. This is in accordance with the statement, which we could make on the basis of ordinary Fourier- analysis in Part I of our paper [3]. Now it is evident that the TQA is suitable for diagnosis of gears.

The other vertical straight lines in Fig. 3 are higher and broken rahmonics of the rotational order of sun gear or annulus resp. The broken rahmonics correspond to higher harmonics of rotational orders in the ordering spectrum, which normally appear as a result of the mentioned faults. The higher rahmonics are generated by the numerical calculation of logarithm of the time–frequency distribution $TFD_X(t;\omega)$ [4]. They are numerically generated artefacts.

The ordering cepstrum at the bottom of Fig. 3 was obtained by averaging of the TQD over time according to equation (5). This averaging could be done without any smearing of peaks because of the data sampling in equidistant angular intervals. Once more we emphasise, that this cepstrum $G_X(\tau)$ is not equal to the Fourier- power cepstrum $C_X(\tau)$ of signal $x(t)$ (see Section 2). But nevertheless, the $G_X(\tau)$ cepstrum can be assessed instead of the real power cepstrum $C_X(\tau)$ because of its similarity. Doing this, the appearance of peaks is a sure indication for periodicities in the appropriate spectra. The cepstral peaks,

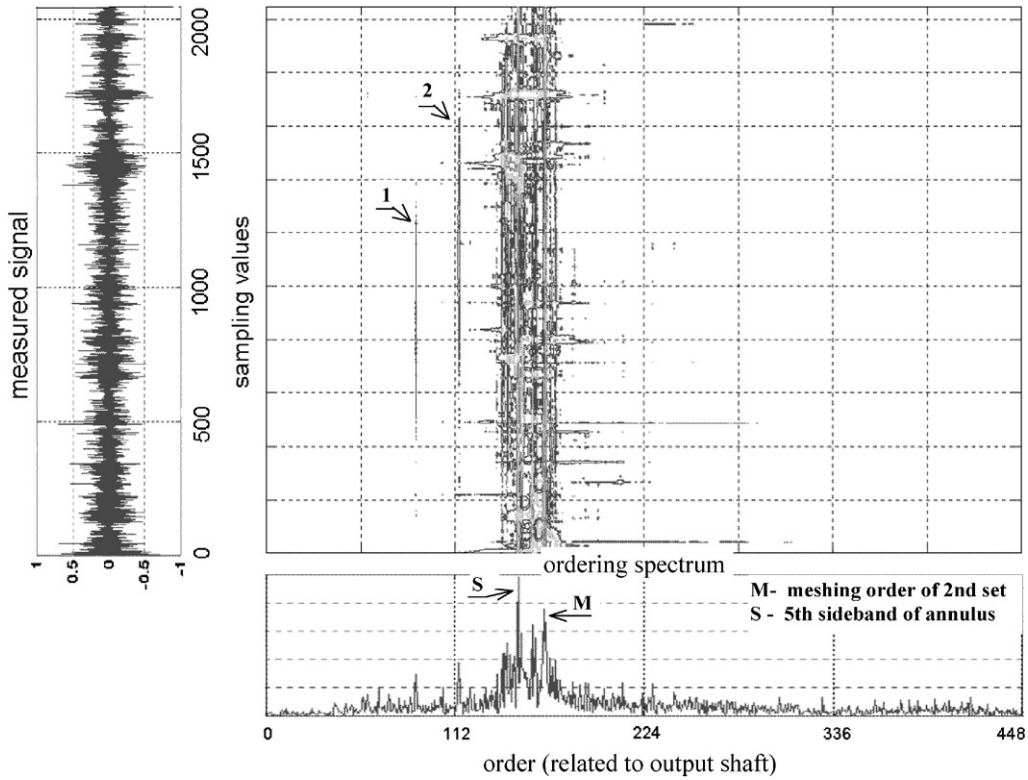

Figure 2. CWD with $\sigma = 0.05$ for three revolutions of the angle-equidistant sampled measuring signal of the gearbox ('1' and '2' mark individual sidebands).

which are caused by faults in sun wheel and annulus, are clearly shown in the ordering cepstrum $G_X(\tau)$ in Fig. 3.

As the result of this section we can state that the angle-equidistant sampled signals seems to be stationary because of the constant angle intervals at the rotating incremental encoder (they can be influenced only by transient resonances during the start up or run down). Therefore, the rotational orders of gear wheels keep constant over the time. As a reflection of this fact, we can consider the perpendicular straight cepstral lines in Fig. 3. In the next section, we will analyse the time-equidistant sampled signals. The result will be inclined cepstral lines in the TQD, whose inclination depends on the changing rate of rotational speed. So we are able to detect the periodicities of sidebands also in the case of quickly changing rotational speed.

3.2. TQA OF TIME- EQUIDISTANT SAMPLED MEASURING DATAS

The measured signal is sampled by the impulses of an electronic generator in equal time intervals. Figure 4 (central part) shows the TFD of one of these signals [3]. Let us repeat once more: the time–frequency transformation was done with the use of a Cohen class transformation with a smoothing kernel, which respects the change of rotational speed. Therefore, the frequency lines with the meshing frequency and its sidebands appear nearly continuously (the discontinuities at the beginning and at the end of the analysed time interval are typical effects of Cohen class). The measured time function and the frequency spectrum over the total measuring time interval are also shown at the left and low margins,

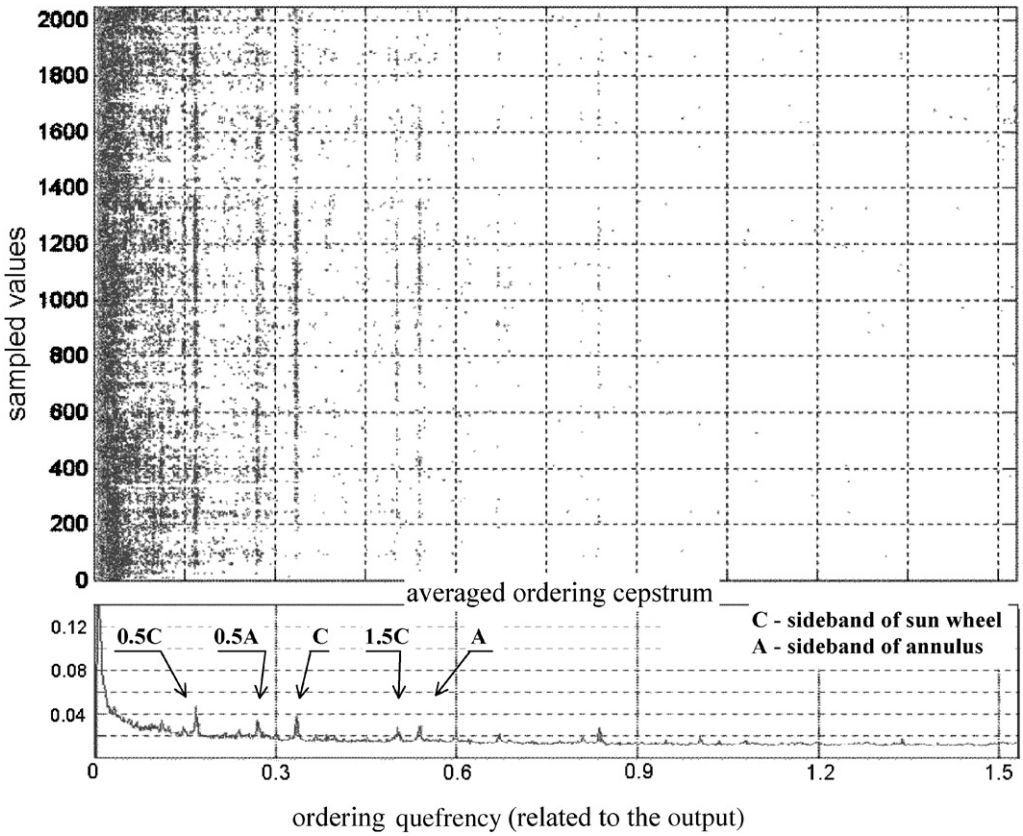

Figure 3. Time–quefrency distribution $TQD_x(t;\tau)$ of the angle-equidistant sampled signal (above) and the averaged ordering cepstrum $G_x(\tau)$ (below).

resp. From this TFD, the time–quefrency transformation was numerically done according to equation (7). The result is shown in Fig. 5. Once more straight lines are orientated nearly perpendicularly. They reflect the distance of sidebands in the time-dependent spectrum (see $TFD_x(t;\omega)$ in Fig. 4). The dominating ones lie at $\tau_{C2} \approx 0.020$ s and $\tau_{A2} \approx 0.032$ s. These quefrencies exactly correspond with time for one revolution of the sun wheel (central gear) and annulus of the second planetary set, resp. Therefore, we can state that they reflect the sidebands, which belong to the damaged wheels.

Nevertheless, all straight lines in Fig. 5 are slightly inclined to the time axis—this is a symptom for the change of rotational speed of the damaged (or badly manufactured) wheels during the measuring time of cca. $T \approx 0.212$ s (three revolutions of output shaft). Because of the insignificance of this inclination, we dared to average the time–quefrency distribution $TQD_X(t;\tau)$ along the time axis according to equation (5) in order to compare the result with the ordering cepstrum, obtained by angle-equidistant sampling. Therefore, we got the appropriate peaks in the cepstral function $G_X(\tau)$—see Fig. 5, low part. Here can we very well recognise the cepstral peaks at quefrencies $\tau_{C2} \approx 0.020$ s and $\tau_{A2} \approx 0.032$ s. These are symptoms for faults or damages at the flanks of sun wheel (marked with 'C') and the annulus (marked with 'A'). Comparing these peaks with the same peaks in Fig. 3 we must state that they are some smeared over because of the weak unstationarity of the sideband distance, of course. But nevertheless a quantitative analysis is able now: by

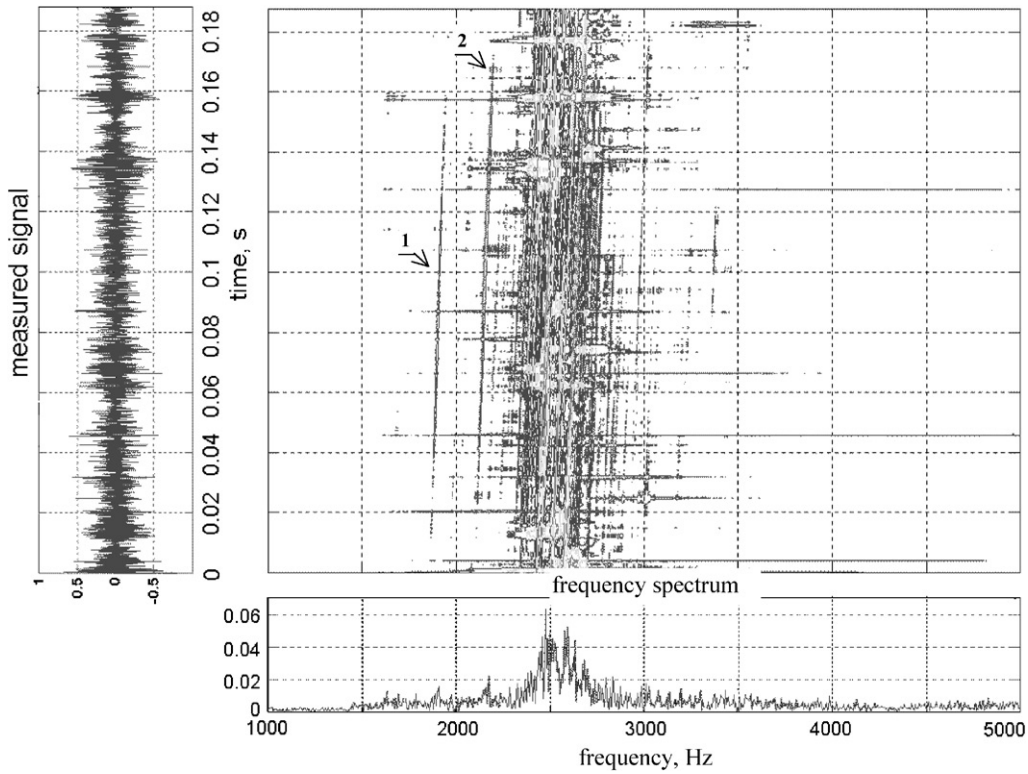

Figure 4. The time–frequency distribution $TFD_x(t;\omega)$ of the time-equidistant sampled measuring signal of gearbox during linear start up (weighted with the acceleration-respecting kernel; '1' and '2' mark individual sidebands).

means of cursor at certain time moments from the contour plot or also by means of the 'averaged' cepstrum at the bottom margin. A better recognition could be reached by averaging along the inclined line of sideband quefrencies.

The apperance of these peaks in the averaged TQD is a clear advantage over the ordinary Fourier-cepstrum (in which these peaks were not recognizable because of the changing rotational speed of the damaged wheels—see Part I of our paper [3]).

Once more we must emphasise that the use of the special smoothing kernel with consideration of the sweeping rotational speed is an indispensable supposition for getting the meaningful TQD according to Fig. 5. For underlining this statement, we calculated the ordinary CWD (its kernel does not respect the time dependence of the rotational speed [5–7]) of the same structure-borne noise during the start up. This CWD ($\sigma = 0.05$) is shown in Fig. 6. This plot is already analysed in Part I of our paper [3]. Figure 7 shows the belonging to TQD. All expected side-band-related cepstral lines (in the TQD) and cepstral peaks (in the averaged cepstrum at the bottom of Fig. 7) are vanished—a consequence of the non-observance of change of rotational speed. This is the promised pragmatic evidence of the unsuitability of the CWD for the recognition of chirps (see Section 5.2 of Part I [3]). Already the analysis of the CWD-plot in Fig. 6 mislead to an undervaluation of the sidebands because of their breaks along the time axis. The final result is a false diagnosis of the technical state of the monitored gear drive.

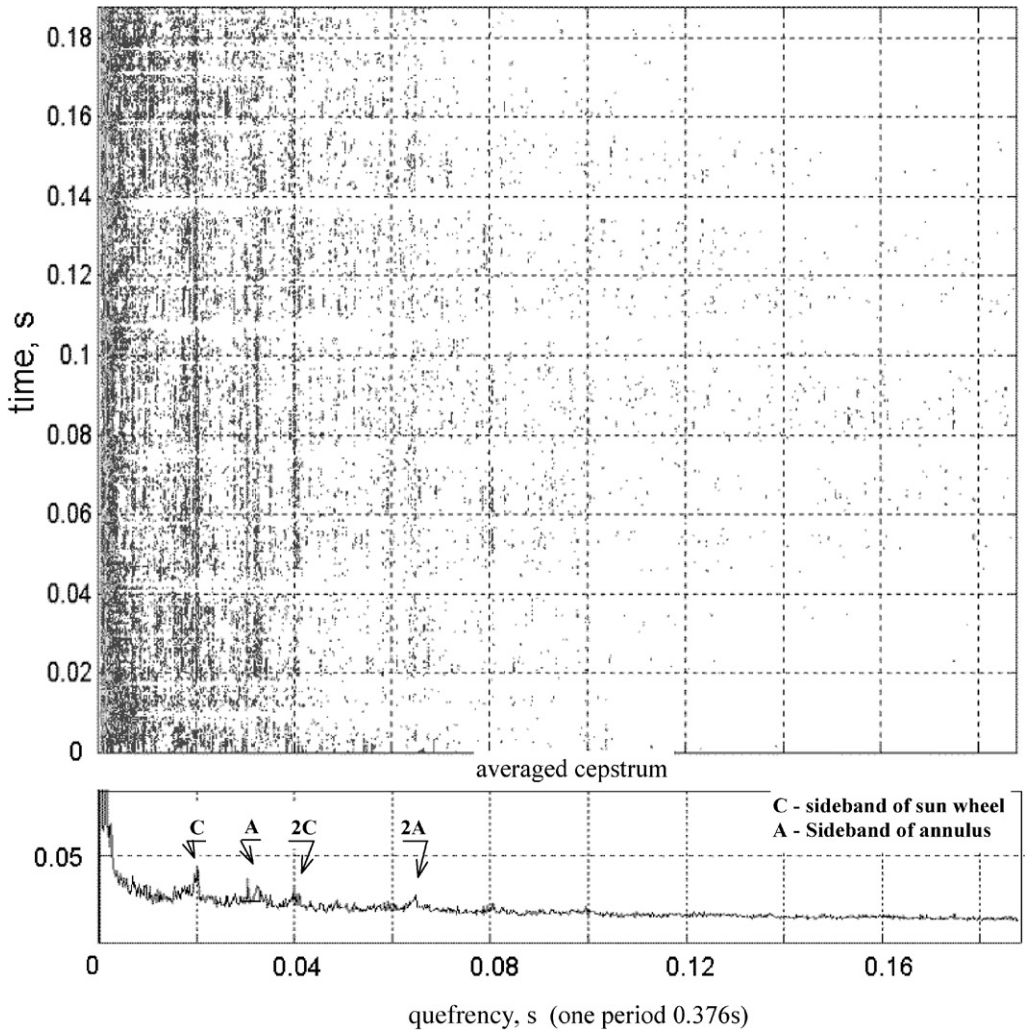

Figure 5. Time–quefrency distribution $TQD_x(t;\tau)$ of the time-equidistant sampled signal, which was calculated outgoing from the time–frequency distribution $TFD_x(t;\omega)$ with the special smoothing kernel $H_C(v;\tau)$ under consideration of angular acceleration (above) and the averaged cepstrum $G_x(\tau)$ (below).

4. SUMMARY

The target of paper in hand is the detection and diagnosis of faults and damages at gear drives under special operational conditions and limited hardware conditions. In contrast to the already known and applied approaches [8–11], we must reach this target by measurement under strong unsteady operational conditions, e.g. during a fast start up or run down. As tools we used the conventional Fourier and cepstral transformations as well as the time–frequency analysis in the special form of time–frequency distributions of Cohen class with different successful results.

While in Part I [3], a new smoothing kernel was created, which respects the change of rotational speed during the measurement; in Part II, we used the time–quefrency

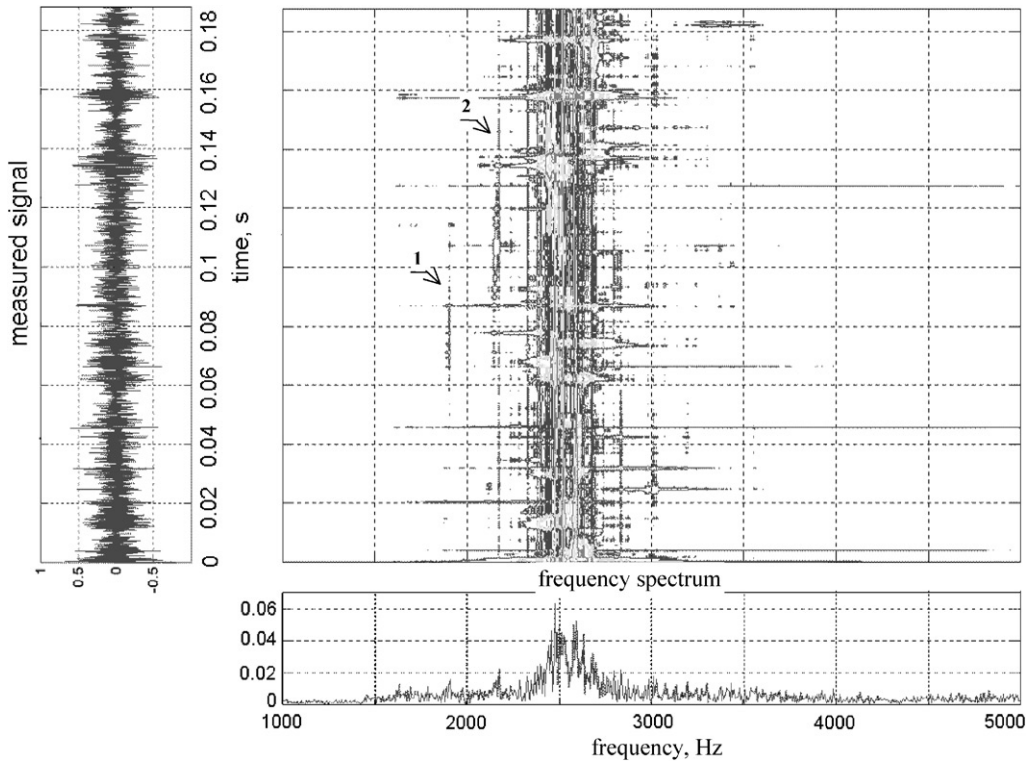

Figure 6. CWD with $\sigma = 0.05$ of the time-equidistant sampled measuring signal of gearbox during linear start up ('1' and '2' mark individual sidebands).

distribution on the basis of the time-dependent cepstral analysis as a improved signal transformation in the time–quefrency domain.

In connection with the mentioned special smoothing kernel distribution and with the given-by Cohen class analysis premise of a good frequency resolution and continously marked sideband lines, the time–quefrency allows the detection and identification of faults and damages, e.g. at tooth flanks of gear wheels, also in the case of instationary rotational speed and without implementation of any incremental sender for rotational angle [1]. This was verified at a planetary gear of passenger car with in-advance-known faults as a case study.

The proposed method for gear-drive monitoring and diagnosis of faults and damages requires much less hardware components compared with the traditional approaches. The disadvantage is a higher demand in numerical computation.

ACKNOWLEDGEMENTS

This research was supported by the Deutscher Akademischer Austauschdienst (DAAD) by awarding the postdoc-scholarship No. A/97/13553. An additional subvention was given by the State Ministry for Sciences and Art of Saxony. We thank Mr. D. Lieske for making the measurements.

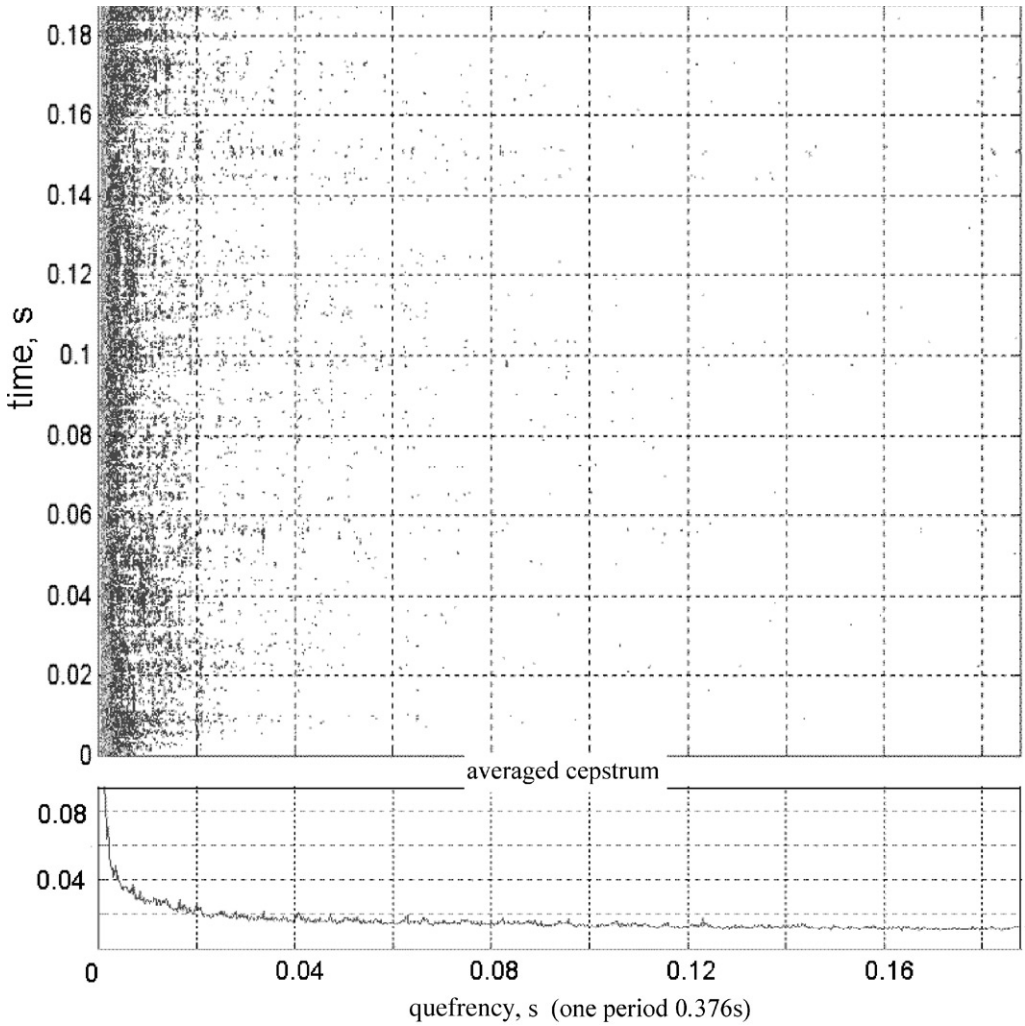

Figure 7. Time–quefrency distribution $TQD_x(t;\tau)$ of the time-equidistant sampled signal, which was calculated outgoing from the ordinary CWD (above) and the averaged cepstrum $G_x(\tau)$ (below).

REFERENCES

1. J. Kolerus 1995 *Zustandsüberwachung von Maschinen*. Sindelfingen: Expert-Verlag.
2. S. Braun 1986 *Mechanical Signature Analysis: Theory and Applications*. New York: Academic Press.
3. G. Meltzer and Yu.Ye. Ivanov 1999 *Mechanical System and Signal Processing* (in print) Fault detection in gear drives with non-stationary rotational speed. Part 1: The time–frequency approach.
4. R. B. Randall *Bruel & Kjaer Application Note* 233-80. Cepstrum analysis and gearbox fault diagnosis.
5. L. Cohen 1989 *Proceedings of the IEEE* **77**, 941–981. Time–frequency distributions—a review.
6. A. Mertins 1996 *Signaltheorie*. Stuttgart: Teubner.
7. F. Hlawatsch and G.F. Bourdeaux-Bartels 1992 *IEEE Signal Processing Magazine* **9**, 21–67. Linear und quadratic time–frequency signal representations.
8. H. Oehlmann, D. Brie, M. Tomczak and A. Richard 1997 *Mechanical System and Signal Processing* **11**, 529–545. A method for analysing gearbox faults using time–frequency representations.

9. W. J. Staszewski, K. Worden and G. R. Tomlinson 1997 *Mechanical System and Signal Processing* **11**, 673–692. Time–frequency analysis in gearbox fault detections using the Wigner–Ville distribution and pattern recognition.
10. F. K. Choy, V. Polyshchuk, R. J. Veillette and M. J. Braun 1997 *International Journal of Turbo and Jet Engines* **14**, 89–97. Health monitoring of a gear transmission using acoustic signatures.
11. M. Hildebrandt and G. Lechner 1992 *Maschinenmarkt, Würzburg* **98**, 42–46. Körperschall-Referenzsignale an Zahnradgetrieben analysieren.